

Optimal Support Solution of Soft Rock Roadway Based on Drucker-Prager Yield Criteria

Minghui Ma

University of Science and Technology Beijing

Qifeng Guo (✉ guoqifeng@ustb.edu.cn)

University of Science and Technology Beijing <https://orcid.org/0000-0003-0904-7342>

Jiliang Pan

University of Science and Technology Beijing

Research Article

Keywords: Roadway, Soft Rock, Optimal Support, Drucker-Prager yield criteria, Elasto-Plastic Analysis

Posted Date: June 10th, 2021

DOI: <https://doi.org/10.21203/rs.3.rs-556392/v1>

License: © ⓘ This work is licensed under a Creative Commons Attribution 4.0 International License.

[Read Full License](#)

1 Optimal Support Solution of Soft Rock Roadway Based on 2 Drucker-Prager Yield Criteria

3 Minghui Ma,^{1,2} Qifeng Guo,^{1*} and Jiliang Pan¹

4 ¹ School of Civil and Resource Engineering, University of Science and Technology Beijing, Beijing 100083,
5 China

6 ² Xilin Gol Shandong Gold Group A'ershada Minerals Co. Ltd., Xinlin Gol, 026000, China

7 *Correspondence should be addressed to Qifeng Guo; guoqifeng@ustb.edu.cn

8 Abstract

9 Through theoretical calculation, the stress and deformation of surrounding rock can be
10 analyzed, which can provide guidance for support design and optimization of soft rock
11 roadway. In this paper, theoretical solutions for both the optimal support pressure and the
12 allowable maximum displacement of surrounding rock are derived based on the Drucker-
13 Prager (DP) yield criteria and the steady creep criterion expressed by the third invariant of
14 deviator stress. The DP criteria with different parameters are compared and analyzed by an
15 engineering example. Then, based on the calculation results, the effects of long-term strength,
16 cohesion and internal friction angle of soft rock on the maximum plastic zone radius and
17 allowable maximum displacement of roadway are discussed. The results show that the optimal
18 support solution of soft rock roadway based on DP criteria can not only reflect the intermediate
19 principal stress reasonably, but also can compare and discuss the influence of different DP
20 criteria on the calculation results. The higher the long-term strength of the roadway surrounding
21 rock is, the smaller the optimal support force is and the larger the allowable maximum
22 displacement is. When the calculated long-term strength of soft rock can ensure that the
23 deformation of the roadway does not exceed the allowable maximum displacement, the
24 roadway can maintain long-term stability without support. With the increase of the cohesion
25 or internal friction angle of soft rock, the radius of plastic zone decreases gradually, and the
26 allowable maximum displacement is reduced by degrees. Through grouting and other means
27 to improve the strength of surrounding rock can effectively reduce the roadway deformation
28 and save support costs.

29 Keywords: Roadway; Soft Rock; Optimal Support; Drucker-Prager yield criteria; Elasto-
30 Plastic Analysis

31 1. Introduction

32 In the process of underground roadway excavation, the stress field will redistribute around the
33 excavation area. The redistribution of stress field leads to convergence deformation of cavities
34 produced by excavation. The size of deformation is related to rock mass properties, in-situ
35 stress and support condition [1-4]. It is important to analyze the distribution of stress field and
36 displacement field of surrounding rock by theoretical calculation [5-7]. Based on the ideal
37 elastic-plastic model, Fenner and Kastner analyzed the elastic and plastic zones of tunnels and
38 derived Fenner formula and Kastner formula [8]. Carranza-Torres [9] proposed an elastic-
39 plastic solution of tunnel problems using the generalized form of the Hoek-Brown failure
40 criterion. Park and Kim [10] discussed the analytical solutions for the prediction of

41 displacements around a circular opening in an elastic–brittle–plastic rock mass compatible with
42 a linear Mohr–Coulomb or a nonlinear Hoek–Brown yield criterion. Sharan [11] presented a
43 simple exact solution for the elastic–brittle–plastic plane strain analysis of displacements
44 around circular openings in an isotropic Hoek–Brown rock subjected to a hydrostatic in-situ
45 stress. According to the strain-softening characteristics of rock mass, Guo et al. [12] and Pan
46 et al. [13] established elastic strain-softening models based on different strength criteria,
47 calculated and analyzed the deformation of roadway surrounding rock, and considered the
48 effects of intermediate principal stress, strain softening parameters and dilatancy. Fan et al.
49 [14] developed a mechanical model for circular tunnels based on the unified strength criterion,
50 and determined the critical support pressure when the plastic zone and damage zone begin to
51 occur.

52 For deep geotechnical engineering, some roadways will gradually transform from shallow hard
53 rock roadway to deep soft rock roadway. Therefore, the problem of soft rock support has
54 become a major safety problem to be solved urgently [15-17]. Soft rock has obvious creep
55 deformation characteristics. In engineering, serious extrusion deformation will occur in all
56 directions of roadway, which will lead to the instability and failure of surrounding rock support
57 structure [18-21]. In the process of support design of soft rock roadway, it is generally
58 necessary to optimize the support parameters reasonably by theoretical calculation, guide
59 engineering design by theoretical calculation results, and reduce the uncertainty brought by
60 engineering analogy method [22-24]. Based on the experience of tunnel engineering and rock
61 mechanics theory, Rabcewicz [25] combined bolt and shotcrete as the main support method,
62 and proposed the new Austrian tunneling method (NATM). At present, NATM is almost a
63 basic method for tunnel excavation in weak and fractured surrounding rock [26-28]. However,
64 NATM is composed of a series of qualitative principles, and there is no quantitative calculation
65 method for the important parameters of support, such as the optimal support force of roadway
66 and the maximum allowable displacement of surrounding rock, which makes the design and
67 construction of support still stay in the stage of engineering experience analogy.

68 According to the creep mechanism of rock and the rheological control principle of soft rock,
69 some scholars have established the optimal support calculation method of soft rock, and solved
70 the optimal support force and the allowable maximum displacement of surrounding rock [29-
71 31]. For example, based on the Mohr-Coulomb (MC) criterion and steady creep criterion
72 expressed by the second invariant of deviator stress, Fan et al. [29] derived the optimal support
73 force and the maximum allowable displacement of surrounding rock for soft rock cavern. Cui
74 et al. [30] discussed the optimum supporting force, the maximum allowable displacement of
75 surrounding rock and the relevant parameters of constant resistance steel frame by using the
76 MC criterion and steady creep criterion expressed by the third invariant of deviator stress.
77 Based on the unified strength theory and considering the effect of the intermediate principal
78 stress and strength criterion, Zeng et al. [31] provided the theoretical solutions of the optimal
79 support force and the maximum allowable displacement of surrounding rock under two kinds
80 of stable creep criteria.

81 The instability of excavation is usually caused by the excessive concentration of stress in the
82 rock mass near the excavation, the excessive stress of supporting components, or the change
83 of rock deformation and strength characteristics [32-36]. And the deformation pressure of
84 viscoelastic rock mass on underground roadway support depends on the properties of
85 surrounding rock and rock-support interaction. Therefore, based on DP series criteria reflecting
86 intermediate principal stress, this paper deduces the analytical solution of optimal support force
87 and allowable maximum displacement of surrounding rock in circular roadway, and compares

88 different DP criteria by an engineering example, and discusses the effects of long-term
 89 strength, cohesion and internal friction angle of soft rock on the maximum plastic zone radius
 90 and allowable maximum displacement of roadway. The research results can provide theoretical
 91 guidance for the rational design and optimization of soft rock roadway support.

92 2. Drucker-Prager Yield Criteria

93 The yield surface of MC yield criterion is an irregular hexagonal pyramid in three-dimensional
 94 stress space. To eliminate the singularity of the yield surface on the cone top and the ridgeline,
 95 Drucker and Prager proposed a smooth conical yield surface that is inscribed in the MC yield
 96 criterion hexagonal pyramid [37]. According to the relative positional relationship between the
 97 DP yield criterion and the Mohr-Coulomb yield criterion on the π plane, the DP yield criteria
 98 are derived [38]. The DP yield criteria can be given by

$$99 \quad \alpha I_1 + \sqrt{J_2} = k \quad (1)$$

100 where the parameters α and k are related to the cohesion c and the internal friction angle φ of
 101 the surrounding rock. According to the matching relationship with the MC criterion, the
 102 corresponding parameter expressions are shown in Table 1. I_1 is the first invariant of stress
 103 tensor, $I_1 = \sigma_1 + \sigma_2 + \sigma_3$; J_2 is the second invariant of stress deviator, $J_2 = [(\sigma_1 - \sigma_2)^2 + (\sigma_2 - \sigma_3)^2 + (\sigma_3 - \sigma_1)^2] / 6$, and σ_1 , σ_2 , and σ_3 are the large, medium and small principal stresses of the surrounding
 104 rock, respectively.
 105

106 The expression of DP criterion under plane strain condition is as follows

$$107 \quad \sigma_1 = M \sigma_3 + N \quad (2)$$

108 where $M = \frac{1+3\alpha}{1-3\alpha}$, $N = \frac{2k}{1-3\alpha}$. Because the internal friction angle φ is always greater than 0,
 109 $\alpha \neq 0$ and $M \neq 1$.

110 Table 1: Parameter expressions of Drucker-Prager yield criteria.

| Serial number | Criterion types | α | k |
|---------------|--|---|--|
| DP1 | The MC criterion based with external corner circumscribed, a circle yield criterion | $\frac{2 \sin \varphi}{\sqrt{3}(3 - \sin \varphi)}$ | $\frac{6c \cos \varphi}{\sqrt{3}(3 - \sin \varphi)}$ |
| DP2 | The MC criterion based with inner corner circumscribed, a circle yield criterion | $\frac{2 \sin \varphi}{\sqrt{3}(3 + \sin \varphi)}$ | $\frac{6c \cos \varphi}{\sqrt{3}(3 + \sin \varphi)}$ |
| DP3 | The MC criterion based with matching circles, for plain strain problems with associated flow rules | $\frac{\sin \varphi}{\sqrt{3}\sqrt{3 + \sin^2 \varphi}}$ | $\frac{3c \cos \varphi}{\sqrt{3}\sqrt{3 + \sin^2 \varphi}}$ |
| DP4 | The MC criterion based with equivalent area, a circle yield criterion | $\frac{2\sqrt{3} \sin \varphi}{\sqrt{2\sqrt{3}\pi} (9 - \sin^2 \varphi)}$ | $\frac{6\sqrt{3}c \cos \varphi}{\sqrt{2\sqrt{3}\pi} (9 - \sin^2 \varphi)}$ |
| DP5 | The MC criterion based with matching circles, for plain strain problems with non-associated flow rules | $\frac{\sin \varphi}{3}$ | $c \cos \varphi$ |

111 3. Optimum Support Calculation of Roadway

112 3.1 Basic assumptions

113 In order to carry out the elastic-plastic analysis of surrounding rock, the following assumptions
114 are made:

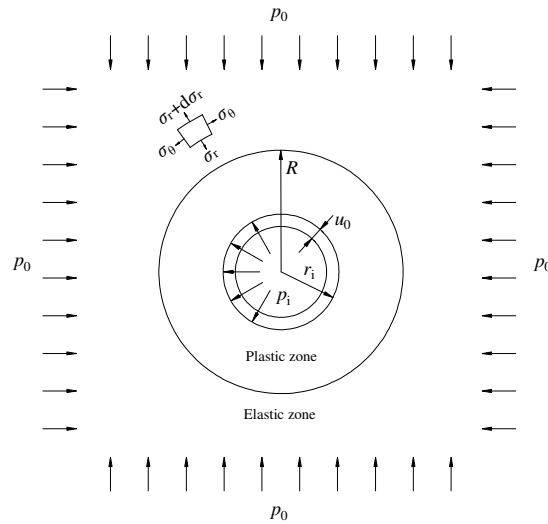
115 (1) The cross-section of the roadway is in circular and the length is infinite. So it can be
116 simplified as a plane strain problem.

117 (2) Surrounding rock of the roadway is a continuous, homogeneous, and isotropic elastic-
118 plastic material.

119 (3) Ignoring the effects of the surrounding rock weight on the yield, the original rock stress can
120 be simplified as a uniform stress distribution. The roadway is under the conditions of uniform
121 in-situ stress and support force.

122 3.2 Elastic-plastic analysis

123 Taking the circular roadway under the combined action of uniform in-situ stress p_0 and uniform
124 support force p_i shown in Figure 1 as an example, the elastic-plastic stresses of surrounding
125 rock during excavation are solved in this section. In Figure 1, r_i is the excavation radius of
126 roadway, R is the radius of plastic zone of surrounding rock, u_0 is the displacement of roadway
127 wall, and σ_r and σ_θ are the radial and tangential stresses respectively.



128

129 Figure 1 Elastic-plastic analysis model of circular roadway [31]

130 In the plastic zone of the surrounding rock, the tangential stress σ_θ and the radial stress σ_r are
131 the maximum and minimum principal stresses, respectively. Equation (2) can be written as

132
$$\sigma_\theta = M \sigma_r + N \quad (3)$$

133 The differential equation of equilibrium for the axisymmetric problem can be expressed as

134
$$\frac{d\sigma_r}{dr} + \frac{\sigma_r - \sigma_\theta}{r} = 0 \quad (4)$$

135 where r is the radius of calculation area of circular roadway.

136 By taking the stress at the inner wall of roadway as the boundary condition, the stress field
137 distribution in plastic zone are obtained as follows [12, 13]

138
$$\left. \begin{aligned} \sigma_r^p &= \left(p_i + \frac{N}{M-1}\right) \left(\frac{r}{r_i}\right)^{M-1} - \frac{N}{M-1} \\ \sigma_\theta^p &= M \left(p_i + \frac{N}{M-1}\right) \left(\frac{r}{r_i}\right)^{M-1} - \frac{N}{M-1} \end{aligned} \right\} \quad (5)$$

139 where p_i is the support force, r_i is the radius of roadway, σ_r^p and σ_θ^p are the radial stress and
140 tangential stress in plastic zone respectively.

141 Assuming that the radial stress at the interface between elastic zone and plastic zone of
142 surrounding rock is σ_r^{e-p} , based on thick-walled cylinder theory [12], the stress field distribution
143 in elastic zone can be obtained as follows

144
$$\left. \begin{aligned} \sigma_r^e &= p_0 - (p_0 - \sigma_r^{e-p}) \frac{R^2}{r^2} \\ \sigma_\theta^e &= p_0 + (p_0 - \sigma_r^{e-p}) \frac{R^2}{r^2} \end{aligned} \right\} \quad (6)$$

145 where p_0 is the uniform in-situ stress, R is the radius of plastic zone, σ_r^e and σ_θ^e are the radial
146 stress and tangential stress in elastic zone respectively, E and ν are elastic modulus and
147 Poisson's ratio of surrounding rock respectively.

148 Since the stress at the elastic-plastic interface of surrounding rock is continuous, the
149 expressions of radial stress at the elastic-plastic interface and the radius of plastic zone can be
150 obtained as follows

151
$$\sigma_r^{e-p} = \frac{2p_0 - N}{M + 1} \quad (7)$$

152
$$R = r_i \left(\frac{\sigma_r^{e-p} + \frac{N}{M-1}}{p_i + \frac{N}{M-1}} \right)^{\frac{1}{M-1}} \quad (8)$$

153 By substituting Equation (7) into Equation (6), the stress solutions in elastic zone are obtained
154 as follows

155

$$\left. \begin{aligned} \sigma_r^e &= p_0 - \frac{(M-1)p_0 + N}{M+1} \left(\frac{2p_0 - N}{M+1} + \frac{N}{M-1} \right)^{\frac{2}{M-1}} \left(\frac{r_i}{r} \right)^2 \\ \sigma_\theta^e &= p_0 + \frac{(M-1)p_0 + N}{M+1} \left(\frac{2p_0 - N}{M+1} + \frac{N}{M-1} \right)^{\frac{2}{M-1}} \left(\frac{r_i}{r} \right)^2 \end{aligned} \right\} \quad (9)$$

156 During the excavation of roadway, the support force of surrounding rock is 0, and the initial
157 plastic zone radius can be calculated by Equation (8). The initial plastic zone radius R_0 is
158 expressed as follows

$$159 \quad R_0 = r_i \left[1 + \frac{(M-1)(2p_0 - N)}{(M+1)N} \right]^{\frac{1}{M-1}} \quad (10)$$

160 In the support stage, the elastic stress solution at the elastic-plastic interface can be obtained
161 by substituting Equation (10) with Equation (9). The radial and tangential stresses at the elastic-
162 plastic interface are as follows

$$163 \quad \left. \begin{aligned} \sigma_r^e |_{r=R_0} &= p_0 - \frac{(M-1)p_0 + N}{M+1} \left[\frac{N}{(M-1)p_i + N} \right]^{\frac{2}{M-1}} \\ \sigma_\theta^e |_{r=R_0} &= p_0 + \frac{(M-1)p_0 + N}{M+1} \left[\frac{N}{(M-1)p_i + N} \right]^{\frac{2}{M-1}} \end{aligned} \right\} \quad (11)$$

164 For the plane strain problem, the Z-direction strain is 0, so the intermediate principal stress σ_z
165 can be derived by Hooke's law as follows

$$166 \quad \sigma_z = \nu(\sigma_\theta + \sigma_r) \quad (12)$$

167 The following equation can be obtained by ordering the principal stresses at the elastic-plastic
168 interface:

$$169 \quad \sigma_1 = \sigma_\theta^e |_{r=R_0}, \quad \sigma_2 = \sigma_z^e |_{r=R_0}, \quad \sigma_3 = \sigma_r^e |_{r=R_0} \quad (13)$$

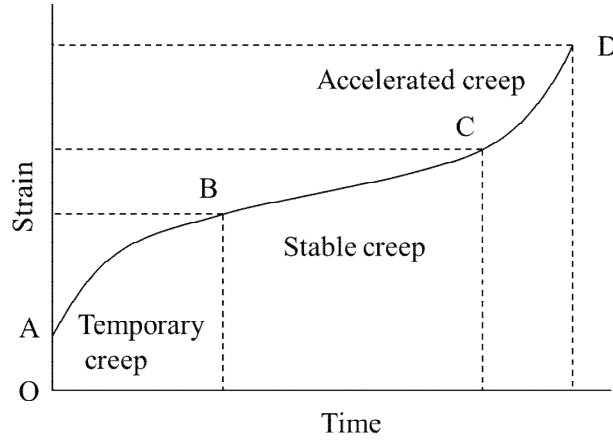
170 Then, combined with equations (11), (12) and (13), the average principal stress σ_m can be
171 obtained as follows

$$172 \quad \sigma_m = \frac{\sigma_1 + \sigma_2 + \sigma_3}{3} = \frac{2(1+\nu)}{3} p_0 \quad (14)$$

173 3.3 Optimal support solution

174 Creep is a special form of elastic-plastic deformation of rock, which is a phenomenon that the
175 strain increases with time under the condition of keeping the stress constant. For example, soft
176 rock or hard rock under high stress usually has obvious creep characteristics, and shows serious
177 extrusion deformation from all directions of underground engineering, which often leads to
178 instability and failure of support [39, 40]. Therefore, this kind of rock can be considered as an

179 elastic-plastic material with rheological properties. The typical creep curve of rock mainly
 180 includes three stages: temporary creep (AB), stable creep (BC) and accelerated creep (CD), as
 181 shown in Figure 2.



182

183

Figure 2 Typical creep curve of rock

184 A large number of engineering practices show that the excessive harmful deformation is the
 185 main reason for the instability of underground engineering. The establishment and application
 186 of creep model is one of the core contents in the study of deformation characteristics of soft
 187 rock. The expression of the steady creep criterion expressed by the third invariant of deviator
 188 stress is as follows [30]

189
$$\sqrt[3]{\frac{27}{2} J_3} \leq \sigma_L \quad (15)$$

190
$$J_3 = (\sigma_1 - \sigma_m)(\sigma_2 - \sigma_m)(\sigma_3 - \sigma_m) \quad (16)$$

191 where σ_L is the long-term strength of rock, J_3 is the third invariant of deviator stress.

192 By substituting Equation (13) and (14) into Equation (15) and making both sides of the
 193 equation equal, the optimum support force of roadway is obtained as follows

194
$$p_{i-\min} = \frac{N}{M-1} \left[\frac{1}{3} \sqrt{\frac{\sigma_L^3}{(1-2\nu)p_0} + (1-2\nu)^2 p_0^2} \left[\frac{N}{M-1} + \left(\frac{M-1}{M+1} \right) p_0 \right]^{-1} \right]^{\frac{M-1}{2}} - \frac{N}{M-1} \quad (17)$$

195 It is the optimal support state when the roadway support force p_i is equal to the optimum
 196 support force $p_{i-\min}$. In this case, the radius of plastic zone is

197
$$R_{\max} = r_i \left[\left(\frac{2p_0 - N}{M+1} + \frac{N}{M-1} \right) \left(p_{i-\min} + \frac{N}{M-1} \right)^{-1} \right]^{\frac{1}{M-1}} \quad (18)$$

198 where R_{\max} is the maximum radius of plastic zone.

199 Based on thick-walled cylinder theory, the displacement in elastic zone is

200
$$u^e = \frac{1+\nu}{E}(p_0 - \sigma_r^{e-p}) \frac{R^2}{r} \quad (19)$$

201 At the elastic-plastic interface, $r=R$, and the displacement of surrounding rock at the elastic-
202 plastic interface is

203
$$u^{e-p} = \frac{(1+\nu)R}{E}(p_0 - \sigma_r^{e-p}) \quad (20)$$

204 In the optimum support condition, the initial elastic displacement at the elastic-plastic interface
205 is as follows

206
$$u_0^e = \frac{(1+\nu)R_{\max}}{E} \frac{(M-1)p_0 + N}{M+1} \quad (21)$$

207 The creep modulus of rock can be obtained by laboratory rheological test. By replacing the
208 elastic modulus E of Equation (21) with the creep modulus E_c , the creep displacement at the
209 elastic-plastic interface can be obtained as follows

210
$$u^c = \frac{(1+\nu)R_{\max}}{E_c} \frac{(M-1)p_0 + N}{M+1} \quad (22)$$

211 The displacement of plastic zone is composed of initial elastic displacement and stable creep
212 displacement. According to Equation (21) and Equation (22), the stable displacement of
213 roadway can be calculated as follows

214
$$\forall u = u^c - u_0^e = \frac{(1+\nu)R_{\max}[(M-1)p_0 + N]}{M+1} \left(\frac{E - E_c}{E \cdot E_c} \right) \quad (23)$$

215 Taking $u|_{r=R_{\max}} = \forall u$ as the displacement boundary condition, the displacement of roadway wall
216 at the optimum support condition is obtained as

217
$$u_{0-\max} = \frac{R_{\max}}{r_i} \forall u = \frac{(1+\nu)R_{\max}^2[(M-1)p_0 + N]}{(M+1)r_i} \left(\frac{E - E_c}{E \cdot E_c} \right) \quad (24)$$

218 It can be seen that different DP yield criteria correspond to different parameters M and N . By
219 substituting Equation (17) into Equation (18) to obtain the maximum radius of plastic zone
220 R_{\max} , and then substituting Equation (18) into Equation (24), the allowable maximum
221 displacement at the roadway wall can be obtained.

222 4 Example Studies and Discussion

223 4.1 Roadway parameters

224 The Beizao Coal Mine is located in Longkou City, Shandong Province, China, which is a
225 typical soft rock mine with complex geological conditions, especially with the continuous
226 extension of mining level, roadway deformation problem is very prominent. Taking the soft
227 rock roadway in the Beizao Coal Mine as an engineering example, the effects of DP criterion

228 and mechanical parameters of surrounding rock on roadway support are analyzed. The
 229 geometric and mechanical parameters of the roadway are shown in Table 2. The yieldable U-
 230 shaped steel ribs are used to support the roadway, and the in-situ measured roadway wall
 231 displacement is 18.7mm.

232 Table 2: Geometrical and mechanical parameters

| Symbol | Description | Value |
|----------------|-------------------------------|-------|
| r/m | Excavation radius | 2.0 |
| p_0/MPa | In-situ stress | 5.6 |
| E/MPa | Elastic modulus | 1500 |
| E_c/MPa | Creep modulus | 400 |
| ν | Poisson's ratio | 0.24 |
| c/MPa | Cohesion | 0.71 |
| $\phi/^\circ$ | Internal friction angle | 23.6 |
| σ_c/MPa | Uniaxial compressive strength | 29.0 |
| σ_L/MPa | Long-term strength | 6.38 |

233 4.2 The effect of yield criteria

234 The calculation results of optimal support force, maximum plastic zone radius and allowable
 235 maximum displacement of surrounding rock under different DP criteria are shown in Table 3.

236 Table 3: Calculation results of different DP yield criteria

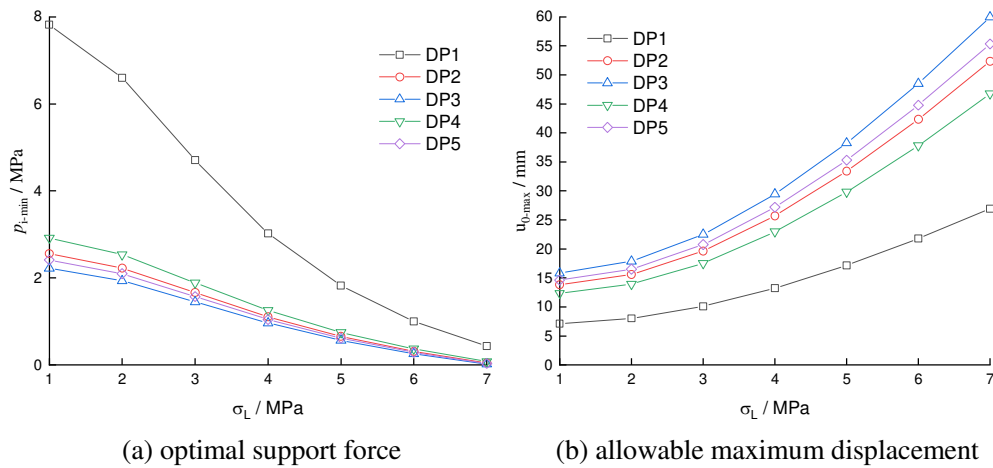
| Serial number | p_{i-min}/MPa | R_{max}/m | u_{0-max}/mm |
|---------------|-----------------|-------------|----------------|
| DP1 | 0.76 | 2.33 | 23.69 |
| DP2 | 0.20 | 3.71 | 46.03 |
| DP3 | 0.16 | 4.06 | 52.72 |
| DP4 | 0.25 | 3.43 | 41.10 |
| DP5 | 0.18 | 3.85 | 48.66 |

237 It can be seen that the optimal support force, maximum radius of plastic zone and allowable
 238 maximum displacement calculated by different DP criteria are different. The optimal
 239 supporting force obtained by DP1 criterion is the largest, while that by DP3 criterion is the
 240 smallest. The optimum support force of DP3 criterion is only 21% of DP1 criterion. The effect
 241 of intermediate principal stress σ_2 on surrounding rock strength is equal to the minimum
 242 principal stress σ_3 according in DP1 criterion, which will exaggerate the influence of
 243 intermediate principal stress. Therefore, the maximum plastic zone radius and allowable
 244 maximum displacement obtained by DP1 criterion are the smallest of DP series criteria. The
 245 maximum plastic zone radius calculated by DP3 criterion is 1.74 times of DP1 criterion, and
 246 the allowable maximum displacement is 2.23 times of DP1 criterion. This means that DP1
 247 criterion and DP3 criterion are the upper and lower limits of DP series criteria respectively.
 248 When DP criteria are used for elastic-plastic analysis of roadway surrounding rock, the
 249 appropriate DP yield criterion should be selected according to the actual engineering
 250 background and the mechanical parameters of surrounding rock.

251 4.3 The effect of long-term strength

252 Figure 3 shows the variation rule of optimal support force and allowable maximum
 253 displacement under different long-term strength. It can be seen that the larger the long-term
 254 strength is, the smaller the optimal support force is and the larger the allowable maximum
 255 displacement is. In other words, the greater the long-term strength of surrounding rock is, the
 256 more stable the roadway is. From Figure 3a, it can be seen that the overall performance of the

257 optimal support force is $DP1 > DP4 > DP2 > DP5 > DP3$. With the increase of the long-term
 258 strength of surrounding rock, the optimal support forces calculated by different DP criteria are
 259 closer and closer, which will eventually completely coincide and achieve the ideal state without
 260 support. The reason for this change is that the larger the long-term strength of rock mass is, the
 261 smaller the plastic zone of roadway is, which leads to the weakening of the effect of yield
 262 criterion. As can be seen from Figure 3b, the allowable maximum displacement is $DP3 > DP5 >$
 263 $DP2 > DP4 > DP1$. The results of DP3 criterion are relatively conservative. Using DP3 criterion
 264 in roadway support design can improve the safety, but it will increase the support cost.



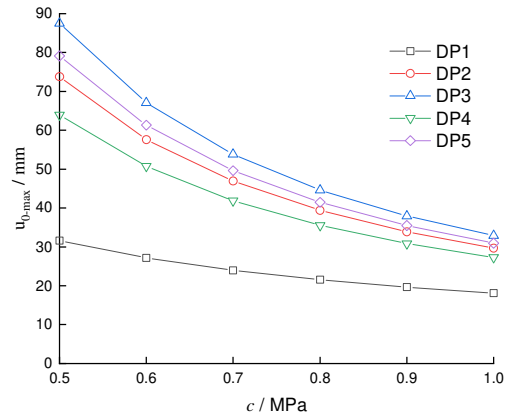
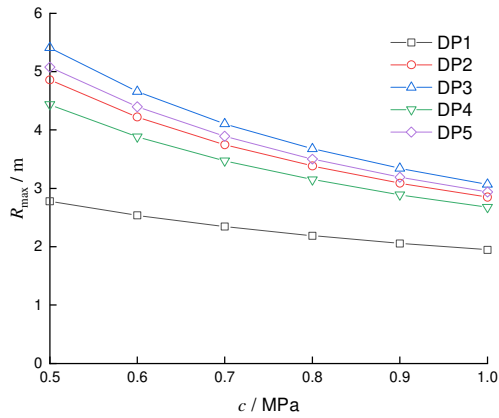
265
266

267 Figure 3 Effect of long-term strength on support

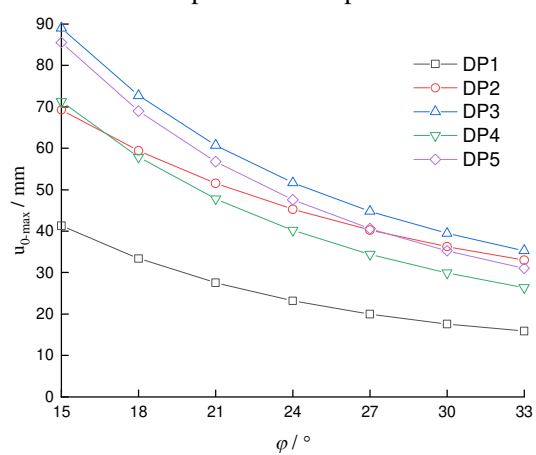
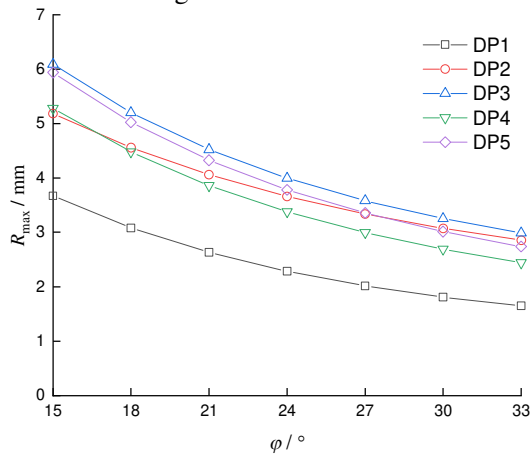
268 **4.4 The effect of strength parameters**

269 Figure 4 and Figure 5 show the variation of maximum plastic zone radius and allowable
 270 maximum displacement under different cohesion and internal friction angles, respectively. It
 271 can be seen that the influence trend of cohesion and internal friction angle on roadway
 272 deformation is roughly the same, that is, with the increase of cohesion or internal friction angle,
 273 the radius of maximum plastic zone is smaller and smaller, and the allowable maximum
 274 displacement is also gradually reduced. The reason for this change is that the increase of
 275 cohesion or internal friction angle increases the bearing capacity of rock mass, thus reducing
 276 the failure range and restraining plastic deformation of surrounding rock.

277 Taking DP1 criterion as an example, when the cohesion increases from 0.5 MPa to 1.0 MPa,
 278 the radius of plastic zone decreases from 2.78 m to 1.95 m, which reduces by nearly 30%. The
 279 allowable maximum displacement was reduced by 43% from 31.58 mm to 18.10 mm. When
 280 the internal friction angle increases from 15 to 33 degrees, the radius of plastic zone decreases
 281 from 3.67 m to 1.65 m, and it decreases by 55%. The allowable maximum displacement is
 282 reduced from 41.30 mm to 15.86 mm, which reduces by 62%. It can be seen that the strength
 283 parameters of rock mass have great influence on roadway support. The mechanical properties
 284 of engineering surrounding rock should be fully considered in support design. For example,
 285 the strength of surrounding rock can be improved by grouting, which can effectively reduce
 286 the deformation of roadway.



(a) plastic zone radius (b) allowable maximum displacement
 Figure 4 Effect of cohesion on radius and maximum displacement of plastic zone



(a) plastic zone radius (b) allowable maximum displacement
 Figure 5 Effect of internal friction angle on radius and maximum displacement of plastic zone

5 Conclusion

(1) An analytical solution of optimal support force and allowable maximum displacement of surrounding rock for circular roadway based on DP series criteria is proposed. The proposed optimal support solution can not only reflect the intermediate principal stress reasonably, but also can compare and discuss the influence of different DP criteria on the calculation results. The analytical solution can also provide theoretical guidance for engineering practice.

(2) The long-term strength of roadway surrounding rock has a significant impact on the optimal support force and the allowable maximum displacement. The higher the long-term strength of roadway surrounding rock is, the smaller the optimal support force is and the larger the allowable maximum displacement is. When the calculated long-term strength of soft rock can ensure that the deformation of the roadway does not exceed the allowable maximum displacement, the roadway can maintain long-term stability without support.

(3) The influence of surrounding rock parameters on roadway support and deformation is also significant. With the increase of cohesion or internal friction angle, the radius of plastic zone of surrounding rock becomes smaller and smaller, and the allowable maximum displacement also decreases gradually. Through grouting and other means to improve the strength of surrounding rock, can effectively reduce the deformation of roadway.

310 **Conflicts of Interest**

311 The authors declare that they have no conflict of interest.

312 **Data Availability**

313 The experimental data used to support the findings of this study are included within the article.

314 **Acknowledgments**

315 Financial support from the Fundamental Research Funds for the Central Universities (Grant
316 No. FRF-IDRY-20-032) and the National Natural Science Foundation of China (No. 51974014)
317 is gratefully acknowledged.

318

319

320 **References**

- 321 [1] Walton, G., Delaloye, D., & Diederichs, M. S. (2014). Development of an elliptical fitting algorithm to
322 improve change detection capabilities with applications for deformation monitoring in circular tunnels
323 and shafts. *Tunnelling and Underground Space Technology*, 43, 336-349.
- 324 [2] Wu, K., Shao, Z., & Qin, S. (2020). An analytical design method for ductile support structures in
325 squeezing tunnels. *Archives of Civil and Mechanical Engineering*, 20(3), 1-13.
- 326 [3] Wu, K., Shao, Z., Qin, S., Zhao, N., & Hu, H. (2020). Analytical-Based Assessment of Effect of Highly
327 Deformable Elements on Tunnel Lining Within Viscoelastic Rocks. *International Journal of Applied*
328 *Mechanics*, 12(03), 2050030.
- 329 [4] Wu, K., Shao, Z., Qin, S., & Li, B. (2020). Determination of deformation mechanism and
330 countermeasures in silty clay tunnel. *Journal of Performance of Constructed Facilities*, 34(1), 04019095.
- 331 [5] Song, F., Wang, H., & Jiang, M. (2018). Analytically-based simplified formulas for circular tunnels
332 with two liners in viscoelastic rock under anisotropic initial stresses. *Construction and Building*
333 *Materials*, 175, 746-767.
- 334 [6] Song, F., Wang, H., & Jiang, M. (2018). Analytical solutions for lined circular tunnels in viscoelastic
335 rock considering various interface conditions. *Applied Mathematical Modelling*, 55, 109-130.
- 336 [7] Pan, J., Guo, Q., Ren, F., & Cai, M. (2019). Comparative analysis of different strength criteria for deep-
337 buried rock roadway under seepage[J]. *Journal of the China Coal Society*, 44(11):3369-3378.
- 338 [8] Xu, S. Q., & Yu, M. H. (2006). The effect of the intermediate principal stress on the ground response
339 of circular openings in rock mass. *Rock Mechanics and Rock Engineering*, 39(2), 169-181.
- 340 [9] Carranza-Torres, C. (2004). Elasto-plastic solution of tunnel problems using the generalized form of
341 the Hoek-Brown failure criterion. *International Journal of Rock Mechanics and Mining Sciences*,
342 41(Suppl. 1), 1-11.
- 343 [10] Park, K. H., & Kim, Y. J. (2006). Analytical solution for a circular opening in an elastic–brittle–plastic
344 rock. *International Journal of Rock Mechanics and Mining Sciences*, 43(4), 616-622.
- 345 [11] Sharan, S. K. (2005). Exact and approximate solutions for displacements around circular openings in
346 elastic–brittle–plastic Hoek–Brown rock. *International Journal of Rock Mechanics and Mining*
347 *Sciences*, 42(4), 542-549.
- 348 [12] Guo, Q., Pan, J., Wu, X., Xi, X., & Cai, M. (2019). A new unified solution for circular tunnels based on
349 generalized SMP criterion considering the strain softening and dilatancy. *Advances in Civil Engineering*,
350 2019.
- 351 [13] Pan, J., Gao, Z., & Ren, F. (2018). Effect of strength criteria on surrounding rock of circular roadway
352 considering strain softening and dilatancy[J]. *Journal of the China Coal Society*, 43(12):3293-3301.
- 353 [14] Fan, H., Wang, L., & Wang, K. (2020). Stability Analysis of Surrounding Rock in Circular Tunnels
354 Based on Critical Support Pressure. *Advances in Civil Engineering*, 2020.
- 355 [15] Yang, X., Pang, J., Liu, D., Liu, Y., Tian, Y., Ma, J., & Li, S. (2013). Deformation mechanism of
356 roadways in deep soft rock at Hegang Xing'an Coal Mine. *International Journal of Mining Science and*
357 *Technology*, 23(2), 307-312.
- 358 [16] Shen, B. (2014). Coal mine roadway stability in soft rock: a case study. *Rock Mechanics and Rock*
359 *Engineering*, 47(6), 2225-2238.

- 360 [17] Yang, S. Q., Chen, M., Jing, H. W., Chen, K. F., & Meng, B. (2017). A case study on large deformation
361 failure mechanism of deep soft rock roadway in Xin'An coal mine, China. *Engineering Geology*, 217,
362 89-101.
- 363 [18] Cao, P., Youdao, W., Yixian, W., Haiping, Y., & Bingxiang, Y. (2016). Study on nonlinear damage creep
364 constitutive model for high-stress soft rock. *Environmental Earth Sciences*, 75(10), 900.
- 365 [19] Wang, J. X., Lin, M. Y., Tian, D. X., & Zhao, C. L. (2009). Deformation characteristics of surrounding
366 rock of broken and soft rock roadway. *Mining Science and Technology (China)*, 19(2), 205-209.
- 367 [20] Wang, Q., Pan, R., Jiang, B., Li, S. C., He, M. C., Sun, H. B., ... & Luan, Y. C. (2017). Study on failure
368 mechanism of roadway with soft rock in deep coal mine and confined concrete support system.
369 *Engineering Failure Analysis*, 81, 155-177.
- 370 [21] Chen, Y., Meng, Q., Xu, G., Wu, H., & Zhang, G. (2016). Bolt-grouting combined support technology
371 in deep soft rock roadway. *International Journal of Mining Science and Technology*, 26(5), 777-785.
- 372 [22] Wang, C., Wang, Y., & Lu, S. (2000). Deformational behaviour of roadways in soft rocks in
373 underground coal mines and principles for stability control. *International Journal of Rock Mechanics
374 and Mining Sciences*, 37(6), 937-946.
- 375 [23] Kang, H. P., Lin, J., & Fan, M. J. (2015). Investigation on support pattern of a coal mine roadway within
376 soft rocks—a case study. *International Journal of Coal Geology*, 140, 31-40.
- 377 [24] Yoshinaka, R., Tran, T. V., & Osada, M. (1998). Non-linear, stress-and strain-dependent behavior of
378 soft rocks under cyclic triaxial conditions. *International Journal of Rock Mechanics and Mining
379 Sciences*, 35(7), 941-955.
- 380 [25] Rabcewicz, L. V. (1965). The new Austrian tunnelling method. *Water Power*, 511-515.
- 381 [26] Fang, Q., Zhang, D., & Wong, L. N. Y. (2012). Shallow tunnelling method (STM) for subway station
382 construction in soft ground. *Tunnelling and Underground Space Technology*, 29, 10-30.
- 383 [27] Li, P., Zhao, Y., & Zhou, X. (2016). Displacement characteristics of high-speed railway tunnel
384 construction in loess ground by using multi-step excavation method. *Tunnelling and Underground
385 Space Technology*, 51, 41-55.
- 386 [28] Luo, Y., Chen, J., Chen, Y., Diao, P., & Qiao, X. (2018). Longitudinal deformation profile of a tunnel
387 in weak rock mass by using the back analysis method. *Tunnelling and Underground Space Technology*,
388 71, 478-493.
- 389 [29] Qiuyan, F., & Weishen, Z. (1997). Method for calculating optimum support of soft rock. *Chinese
390 Journal of Geotechnical Engineering*, 19(2), 77-83.
- 391 [30] Cui, X. H., Gao, Y. F., Fan, Q. Z., & Niu, X. L. (2006). Optimum calculating method for constant
392 resistant supporting of roadway surrounding rock. *Chinese Journal of Geotechnical Engineering*, 28(5),
393 674-678.
- 394 [31] Zeng, K., Yang, W., Zhang, C., & Dai, H. (2018). Optimal Support in Soft Rock Tunnel Based on the
395 Unified Strength Theory and Steady Creep Guideline. *Advanced Engineering Sciences*, 50(01):62-70.
- 396 [32] Filcek, H., & Kwaśniewski, M. A. (1993). Fundamentals of Mine Roadway Support Design: Rock–
397 Support Interaction Analysis. In *Analysis and Design Methods*, Pergamon, 671-699.
- 398 [33] Pan, J., Wu, X., Guo, Q., Xi, X., & Cai, M. (2020). Uniaxial experimental study of the deformation
399 behavior and energy evolution of conjugate jointed rock based on AE and DIC methods. *Advances in
400 Civil Engineering*, 2020.
- 401 [34] Guo Q, Pan J, Cai M, et al. Analysis of Progressive Failure Mechanism of Rock Slope with Locked
402 Section Based on Energy Theory[J]. *Energies*, 2020, 13(5): 1128.
- 403 [35] Guo Q, Pan J, Cai M, et al. Investigating the effect of rock bridge on the stability of locked section
404 slopes by the direct shear test and acoustic emission technique[J]. *Sensors*, 2020, 20(3): 638.
- 405 [36] Xi, X., Wu, X., Guo, Q., & Cai, M. (2020). Experimental investigation and numerical simulation on the
406 crack initiation and propagation of rock with pre-existing cracks. *IEEE Access*, 8, 129636-129644.
- 407 [37] Alejano, L. R., & Bobet, A. (2012). Drucker–Prager criterion. In *The ISRM Suggested Methods for
408 Rock Characterization, Testing and Monitoring: 2007-2014* (pp. 247-252). Springer, Cham.
- 409 [38] Jiang, H., & Xie, Y. (2011). A note on the Mohr–Coulomb and Drucker–Prager strength criteria.
410 *Mechanics Research Communications*, 38(4), 309-314.
- 411 [39] Chu, Z., Wu, Z., Liu, Q., & Liu, B. (2020). Analytical Solutions for Deep-Buried Lined Tunnels
412 Considering Longitudinal Discontinuous Excavation in Rheological Rock Mass. *Journal of Engineering
413 Mechanics*, 146(6), 04020047.
- 414 [40] Chu, Z., Wu, Z., Liu, B., & Liu, Q. (2019). Coupled analytical solutions for deep-buried circular lined
415 tunnels considering tunnel face advancement and soft rock rheology effects. *Tunnelling and
416 Underground Space Technology*, 94, 103111.

Figures

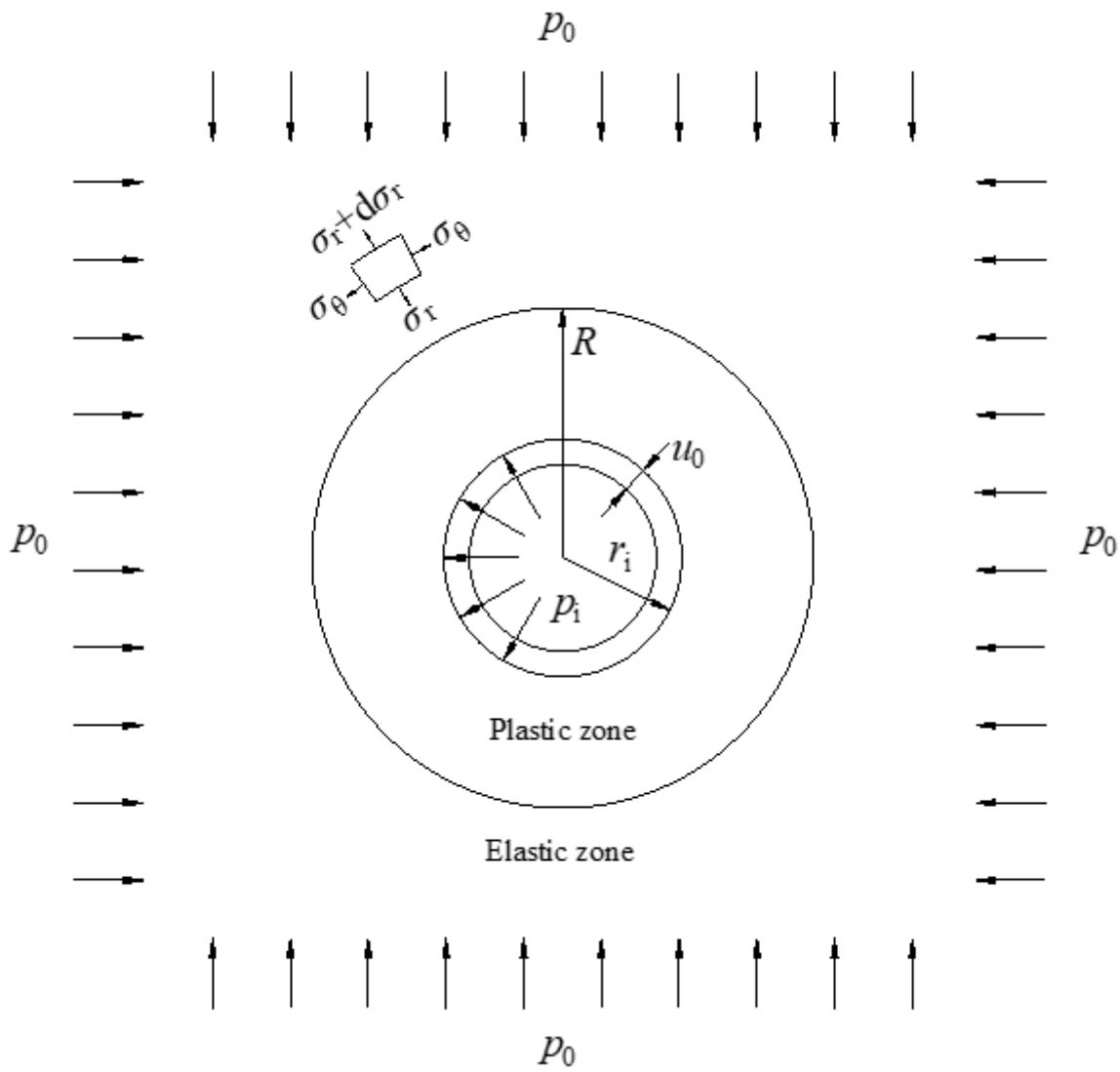


Figure 1

Elastic-plastic analysis model of circular roadway [31]

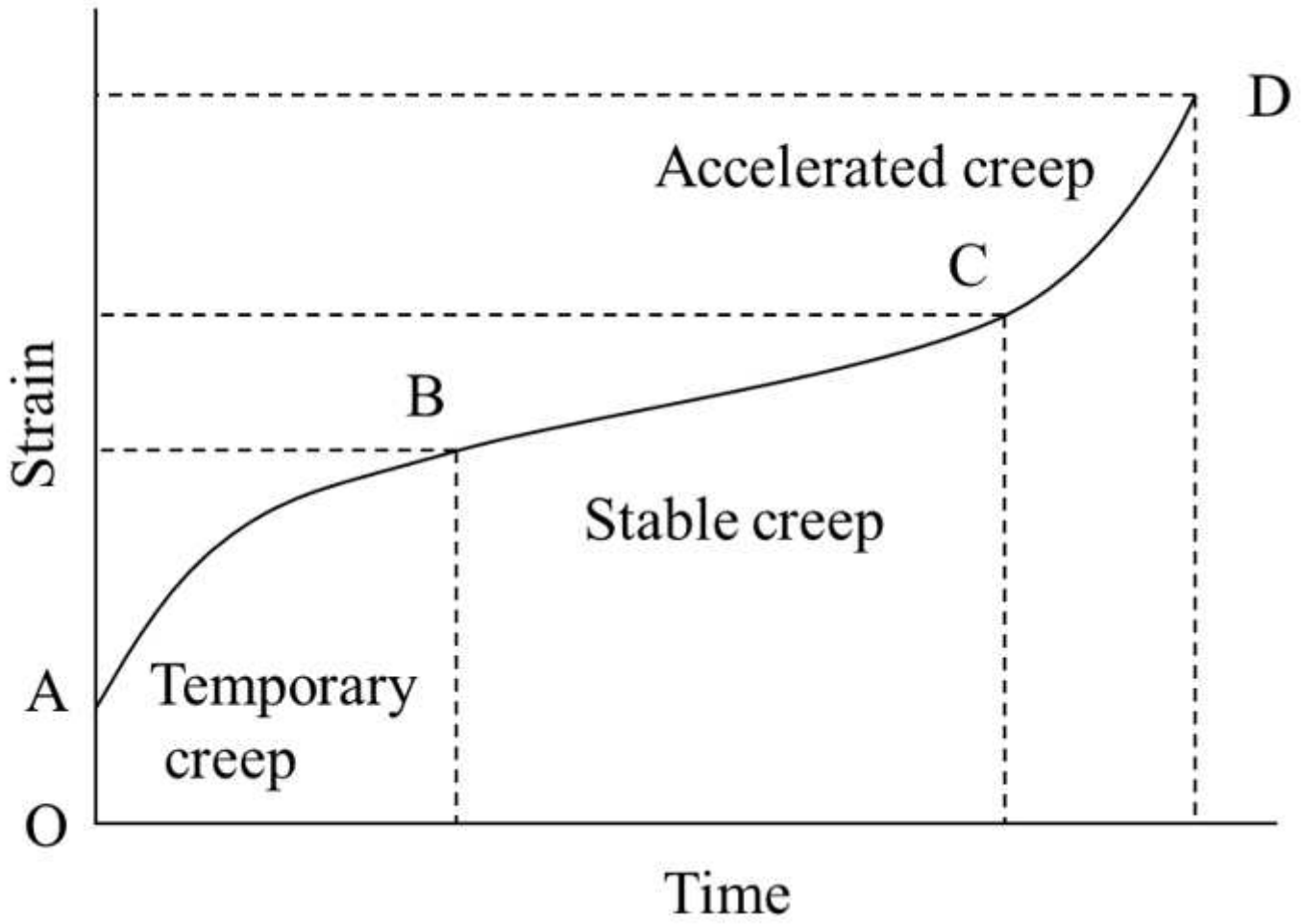
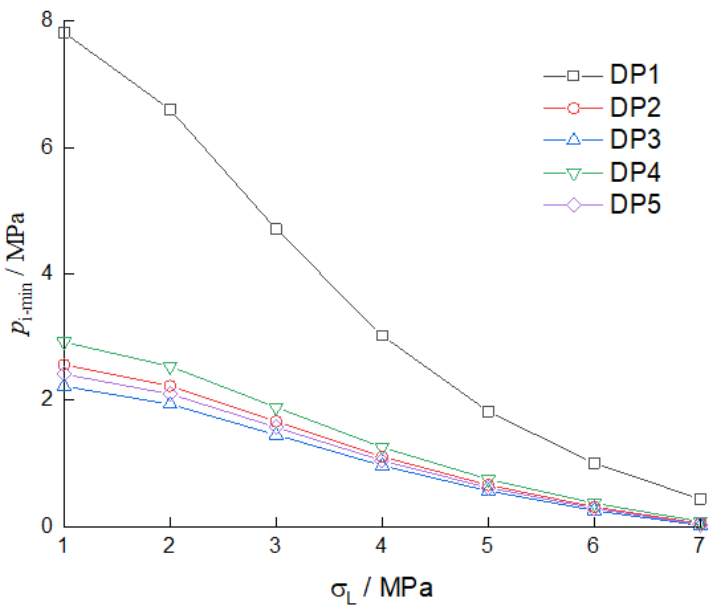
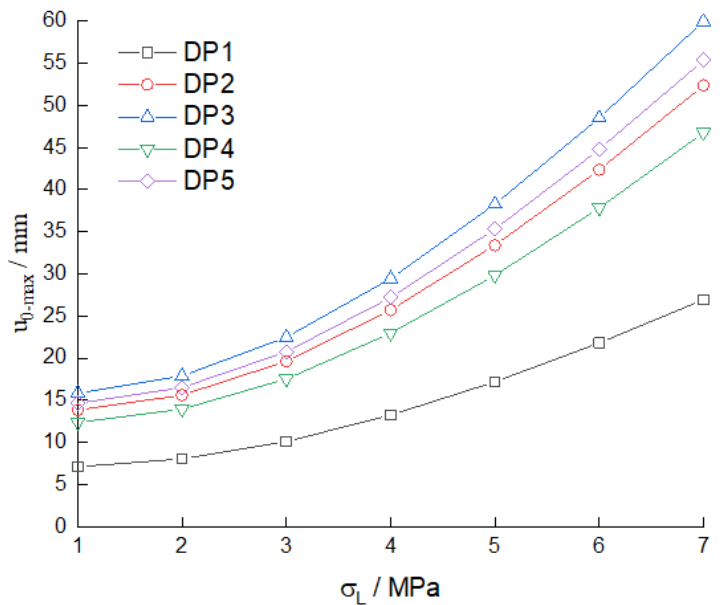


Figure 2

Typical creep curve of rock



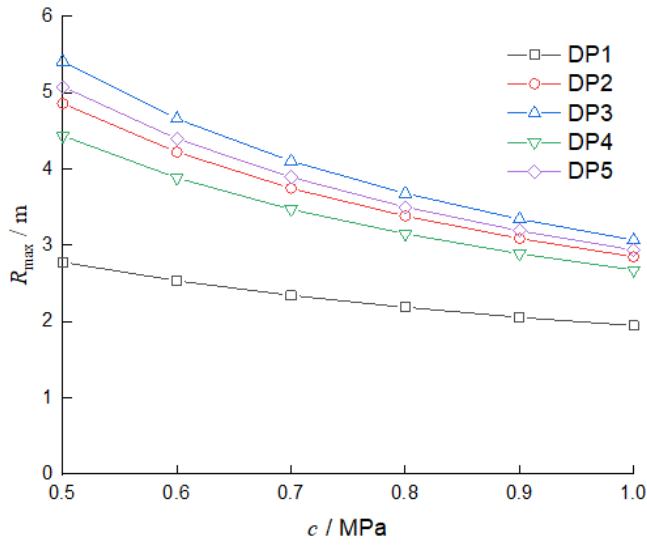
(a) optimal support force



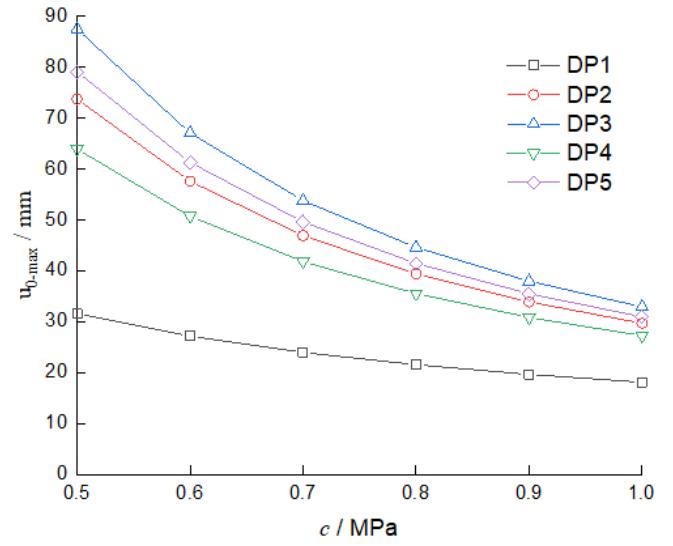
(b) allowable maximum displacement

Figure 3

Effect of long-term strength on support



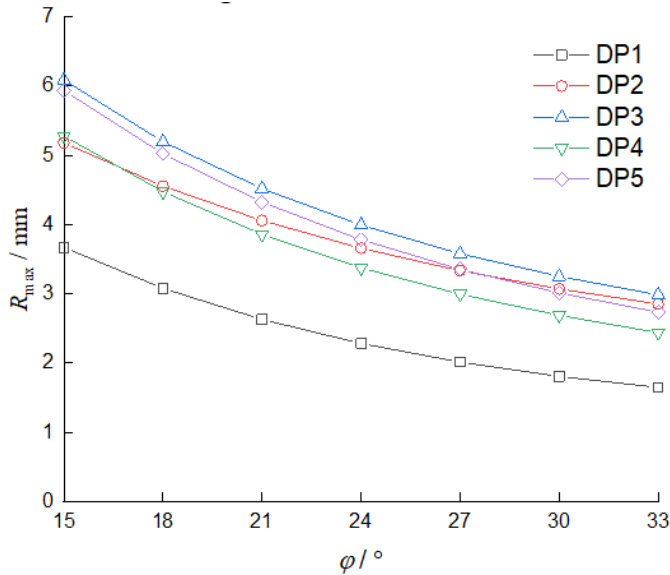
(a) plastic zone radius



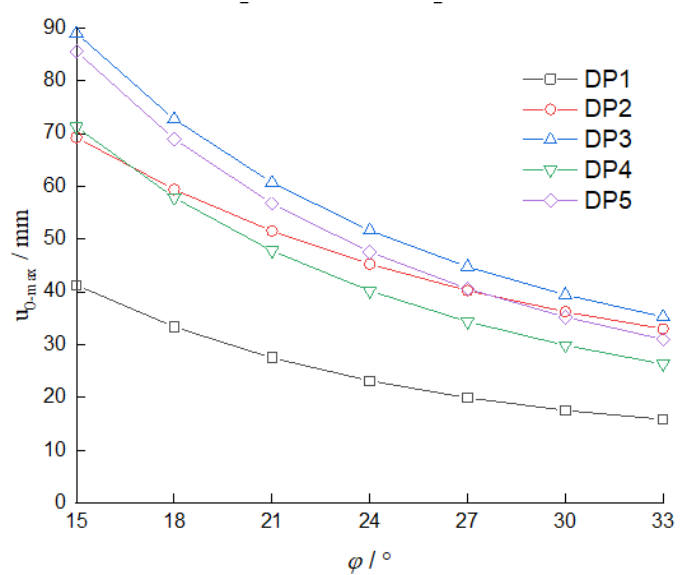
(b) allowable maximum displacement

Figure 4

Effect of cohesion on radius and maximum displacement of plastic zone



(a) plastic zone radius



(b) allowable maximum displacement

Figure 5

Effect of internal friction angle on radius and maximum displacement of plastic zone